


 Cite this: *RSC Adv.*, 2024, 14, 20660

# Fractionation of beech wood cell walls into digestible cellulose-rich residues and photoluminescent lignin-rich precipitates *via* semi-flow hot-compressed water treatment with 2-naphthol†

 Masatsugu Takada, <sup>a</sup> Yutaka Okazaki, <sup>b</sup> Shinya Kajita, <sup>a</sup> Haruo Kawamoto <sup>b</sup> and Takashi Sagawa <sup>b</sup>

Utilization of cell wall components of woody biomass has attracted attention as alternatives for fossil fuels towards a sustainable society. A semi-flow hydrothermal treatment was used to fractionate the beech (*Fagus crenata*) wood into cellulose-rich residues and lignin-rich precipitates. The enzymatic saccharification of the cellulose component in the residue was enhanced significantly because the preferential delignification from the secondary wall increased enzyme accessibility. Meanwhile, the precipitated lignin was soluble in organic solvent and exhibited clear photoluminescence (PL) according to the chromophore distances. Furthermore, the carbocation scavenger, 2-naphthol, was impregnated into the beech wood to inhibit the lignin re-condensation reaction. As a result, the digestibility of the cellulose component in the residue increased because unproductive enzymatic binding of lignin and lignin re-condensation were both suppressed. In addition, the PL intensity of the precipitates was significantly enhanced, indicating that 2-naphthol bound to the lignin molecules influenced the PL properties. Overall, fractionation using a semi-flow hydrothermal treatment efficiently uses both polysaccharides and lignin, especially the impregnation of 2-naphthol provided advantages for both saccharides and lignin. Monosaccharides can be converted into valuable products *via* a sugar platform, and the lignin precipitates exhibit useful PL properties that give them significant potential as a feedstock for numerous valuable materials, such as fluorescence reagents and spectral conversion agents. The results presented herein provide insights that are crucial for the comprehensive utilization of cell wall components for sustainable biorefinery systems.

 Received 26th April 2024  
 Accepted 20th June 2024

DOI: 10.1039/d4ra03094j

[rsc.li/rsc-advances](https://rsc.li/rsc-advances)

## Introduction

Carbon-neutral woody biomass resources are attracting attention as alternatives for fossil fuels to promote a sustainable society. The cell walls of woody resources consist of polysaccharides (*e.g.*, cellulose and hemicellulose) and aromatic polymers (*e.g.*, lignin). The polysaccharides have a wide application scope, including in pulp & paper, medicine, film, and food products. Notably, cellulose can be converted into glucose *via* enzymatic saccharification, and the glucose can be further converted into value-added products through a well-established

sugar platform.<sup>1</sup> In contrast, lignin is difficult to use because of its complex and heterogenous structure. In general, most lignin by-products from paper mills are used as a heat source, and this process is expected to convert lignin to more valuable materials.<sup>2</sup> Importantly, lignin has the potential to serve as an optical material owing to its large molar extinction coefficient. For example, lignin was mixed with a polymer and used as an ultraviolet (UV) absorber.<sup>3–5</sup> Our group previously demonstrated that the photoluminescence (PL) properties of lignin in solution and in films could be controlled by modulating the distance between chromophores of lignin.<sup>6</sup> This indicated that lignin could be used as a feedstock for valuable materials, such as fluorescence reagents and optical wavelength conversion agents.

Polysaccharides and lignin have distinct applications, which means that the fractionation of these components is crucial to enable utilization of the entire cell walls from woody biomass. Semi-flow hot-compressed water (HCW) treatment (150–230 °C/10 MPa) can be applied to fractionate the cell wall components

<sup>a</sup>Graduate School of Bio-Applications and Systems Engineering (BASE), Tokyo University of Agriculture and Technology, 2-24-16, Nakacho Koganeishi, Tokyo 184-8588, Japan. E-mail: [takada-masatsugu@go.tuat.ac.jp](mailto:takada-masatsugu@go.tuat.ac.jp)

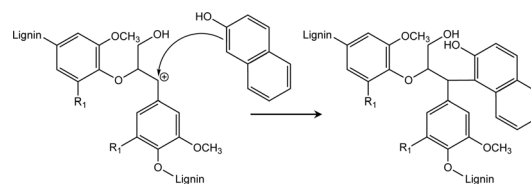
<sup>b</sup>Graduate School of Energy Science, Kyoto University, Yoshida-Honmachi, Sakyo-ku, Kyoto, 606-8501, Japan

† Electronic supplementary information (ESI) available. See DOI: <https://doi.org/10.1039/d4ra03094j>



under relatively mild conditions without a catalyst.<sup>7,8</sup> This system does not require any post-treatment of the catalyst (*e.g.*, neutralization) or recovery of solvents, and therefore, it is expected to be a “green” system. Another advantage of the semi-flow type reactor is the suppression of undesirable reaction of decomposed products due to its short residence time. When Japanese beech (*Fagus crenata*) underwent a semi-flow HCW treatment, most of the hemicellulose and more than half of the lignin were dissolved in the HCW-soluble portion, while cellulose remained as an insoluble residue with some additional residual lignin. Within the HCW-soluble portion, some of the liquefied products could be precipitated after 12 h standing under ambient conditions, and these precipitates were mostly composed of lignin.<sup>9</sup> Among three fractionated components (*i.e.*, insoluble residue, precipitates, and water-soluble portion), the water-soluble portion was analyzed in detail, and the potential application was proposed such as the valorization of them into acetic acid *via* anaerobic microbe.<sup>10</sup> In contrast, the applications of cellulose-rich insoluble residue and lignin-rich precipitates has not yet been explored. In terms of their utilizations, it is expected that the cellulose-rich insoluble residue can be converted into glucose through enzyme-mediated bioconversion. In contrast, lignin-rich precipitates may have potential as feedstocks for luminescent materials.

During the enzyme-mediated bioconversion of lignocelluloses, lignin inhibits enzymatic hydrolysis through two predominant mechanisms (*i.e.*, unproductive binding of enzymes and restriction of fiber swelling), thereby limiting enzyme access to the cellulosic components.<sup>11</sup> Moreover, recondensation of lignin occurs under acidic conditions, which increases the molecular weight and hydrophobicity of lignin, while reducing its digestibility. The key structures during lignin recondensation under acidic conditions are the carbocation intermediates generated on the lignin side chains following the cleavage of  $\beta$ -aryl ether linkages (Scheme 1). The electrophilic carbocation forms stable C–C bonds, resulting in the production of phenylcoumaran and resinol.<sup>12</sup> Pielhop *et al.* and Wayman *et al.* added carbocation scavengers before the acidic pretreatment and reported mitigation of the lignin recondensation, as well as significantly increased conversion yields (Scheme 2).<sup>12,13</sup> Among the potential carbocation scavengers, 2-naphthol exhibits strong PL because of its long-conjugated structure. Therefore, it is expected that 2-naphthol-incorporated lignin would have unique PL properties. We hypothesized that the incorporation of 2-naphthol before the semi-flow HCW treatment would have dual functionality: increasing the digestibility of the insoluble residue and



Scheme 2 Reaction mechanism of the nucleophilic attack of 2-naphthol on a carbocation formed under acidic conditions.<sup>13</sup>

enhancing the PL properties of the precipitates. Since 2-naphthol is commonly used for the preparation of a wide range applications such as antiseptics, pharmaceuticals and dyes, it is a practical reagent for the biorefinery system. However, it is noted that 2-naphthol in monomeric form is toxic to aquatic organisms and blood circulation in humans.<sup>14,15</sup>

In the present study, beech wood was treated *via* semi-flow HCW and fractionated into insoluble cellulose-rich residues and lignin-rich precipitates. The enzyme-mediated digestibility of the cellulose components in the residue and the enzyme accessibility to cellulose were evaluated based on enzyme cocktails, water retention values (WRVs), and Simon's staining. The results indicated that the distribution of lignin within the cell wall affects the digestibility.<sup>16,17</sup> Therefore, the lignin distribution and the surface morphology of the insoluble residue were observed using microscopic techniques. Additionally, the optical properties of the lignin-rich precipitates in solution and in films were analyzed based on their UV-vis absorbance and PL spectra. In addition, 2-naphthol was impregnated into beech wood prior to the semi-flow HCW treatment, which fractionated the cellulose-rich insoluble residue and lignin-rich precipitates. The impacts of 2-naphthol on both the digestibility of the cellulose component and the PL properties of the lignin-rich precipitates were analyzed.

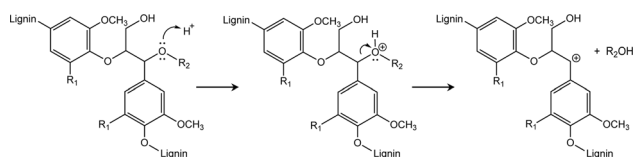
## Materials and methods

### Biomass and chemicals

The sapwood of Japanese beech was milled in a Wiley mill (Thomas Scientific, NJ, USA), and the obtained flour was sieved with mesh screens to collect particles between 0.15 and 1.0 mm. The sieved flour was extracted with acetone in a Soxhlet apparatus and dried at 105 °C for 24 h prior to the experiments. The milled wood lignin (MWL) was prepared by ball milling and extraction with 1,4-dioxane according to an established procedure.<sup>18</sup> Poly(methyl methacrylate) (PMMA) and polyhydroxyethyl methacrylate (PHEMA) were purchased from Sigma-Aldrich Co. LLC. All other chemicals used in this study were of reagent grade, purchased from Nacalai Tesque, Inc. (Kyoto, Japan), and used without further purification.

### Hot-compressed water treatment and fractionation

For the HCW treatment, approximately 0.5 g of oven-dried extractive-free beech flour was placed in a reaction vessel, as described in a previous report.<sup>9</sup> The reaction was carried out at 230 °C/10 MPa for 15 min, during which time, most of the



Scheme 1 Formation of carbocation on a representative lignin structure under acidic conditions ( $R_1 = \text{H}$  or  $\text{OCH}_3$ ,  $R_2 = \text{Ar}$ ).<sup>13</sup>



hemicellulose and some of the lignin could be solubilized. The obtained HCW-soluble portion was allowed to stand for 12 h under ambient conditions to allow for precipitate formation (Fig. S1†). The mixture was then filtered through a Millipore polytetrafluoroethylene membrane filter paper (pore size = 0.45  $\mu\text{m}$ ) to isolate the precipitates. The insoluble residues remaining in the reaction vessel were washed with water and dried at 105  $^{\circ}\text{C}$  for 12 h to determine the oven-dried weight. The chemical compositions of the initial biomass and each fraction were analyzed in triplicate according to TAPPI standard T-22 om-88 method. The chemical composition of the untreated beech wood is shown in Table 1.

### Analytical methods for the insoluble residue

Enzymatic hydrolysis of the insoluble residue was performed using 2 mL centrifuge tubes containing a cellulase enzyme cocktail: Cellic CTec2 (Novozymes, Davis, CA, USA),  $\beta$ -glucosidase, xylanase, and acetate buffer (50 mM, pH 4.8) at a 2% solid loading. The enzyme loading was 60 mg CTec2, 30 mg  $\beta$ -glucosidase, and 30 mg xylanase per gram of cellulose. The tubes were incubated at 50  $^{\circ}\text{C}$  for 72 h. The obtained glucose was quantified by high-performance liquid chromatography, and the cellulose conversion yields were calculated according to the obtained glucose yields and the cellulose content in the substrates. When performing hydrolysis with bovine serum albumin (BSA), samples were impregnated with acetate buffer (50 mM, pH 5.0) containing 10 mg mL<sup>-1</sup> BSA at room temperature overnight before adding enzymes. The WRVs of the insoluble residue were measured in triplicate using a WRV unit equipped with a 200 mesh screen, according to TAPPI Useful Method-256. Simon's staining was conducted according to the method described by Chandra *et al.*<sup>19</sup> using high molecular weight Direct Orange 15 (DO) dye.

Table 1 Chemical composition of beech wood and yields of each fraction obtained after treating beech wood *via* semi-flow hot-compressed water

Chemical composition of beech wood and components in each fraction	Yield (initial biomass-based wt%)
<b>Chemical composition</b>	
Cellulose	48.5
Hemicellulose	25.5
Lignin	25.3
Protein	<0.1
Inorganics	0.6
<b>Insoluble residue</b>	
Cellulose	39.5 $\pm$ 0.6
Hemicellulose	27.6 $\pm$ 0.5
Lignin	1.8 $\pm$ 0.1
	10.0 $\pm$ 0.2
<b>Precipitates</b>	
Cellulose	6.8 $\pm$ 0.7
Hemicellulose	0.3 $\pm$ 0.1
Lignin	0.3 $\pm$ 0.1
	6.1 $\pm$ 0.6
<b>Water-soluble portion (others)</b>	
	53.7 $\pm$ 0.3

Scanning electron microscopy (SEM; SU-6600, Hitachi High-Technologies Corporation, Tokyo, Japan) was used to observe the surface morphology of the insoluble residues. Freeze-dried substrates were placed on an SEM stub, followed by gold-coating. In addition, the lignin distribution within the cell wall was observed using UV microscopy. The residues were embedded in an epoxy resin, and the embedded samples were cut into sections (thickness = 0.5  $\mu\text{m}$ ) using a diamond knife and mounted on an ultramicrotome. Each section was placed on a quartz slide before analysis with an MSP-800 (Carl Zeiss, Oberkochen, Germany) at a wavelength of 280  $\pm$  5 nm.<sup>20</sup>

### Analytical methods for the precipitates

The precipitates were dissolved in *N,N*-dimethylformamide (DMF) and chloroform (CHCl<sub>3</sub>) at 10 mg mL<sup>-1</sup>. Their UV-vis absorption and PL spectra were recorded with V-650 (Jasco Co., Ltd, Tokyo, Japan) and FP-8600 (Jasco Co., Ltd, Tokyo, Japan) instruments, respectively. Gel permeation chromatography (GPC) was performed using an LC-10A instrument (Shimadzu, Kyoto, Japan) under the following specifications: Column, Shodex KF-801 + KF-802 + KF-802.5 + KF-803 (Showa Denko, Tokyo, Japan); eluent, tetrahydrofuran (THF); flow rate, 0.6 mL min<sup>-1</sup>; column temperature, 50  $^{\circ}\text{C}$ ; detector, UV light at 280 nm. Polystyrene standards were used for comparison. Before GPC analysis, lignin was acetylated to improve its solubility in THF in accordance with an established method.<sup>21</sup> Fourier transform infra-red (FT-IR) spectra of precipitated lignin were recorded using the KBr pellet method (IRAffinity-1S instrument, Shimadzu Co., Kyoto, Japan).

## Results and discussion

### Fractionation of cell wall components *via* semi-flow hot-compressed water

After treating beech wood using the semi-flow HCW technique, the yields of the water insoluble residue, water-soluble portion, and precipitates were computed (Table 1). Approximately 60% of the cell wall components were decomposed and eluted in the HCW, while 39.5% remained as the insoluble residue. After the 12 hours sedimentation step, 6.8% of the HCW-soluble portion was retrieved as precipitates, while the remaining 53.8% was obtained as the water-soluble portion. The insoluble residue contained mainly cellulose, although some lignin remained. In contrast, the precipitates mainly comprised lignin. The lignin structure of the precipitates was similar to that of MWL, with abundant ether linkages, indicating that it had undergone limited structural changes.<sup>9</sup> Hemicellulose-derived saccharides, such as xylo-oligosaccharides, and some cellulose-derived saccharides were isolated from the water-soluble portion. In addition, lignin-derived monomers, such as coniferyl alcohol and sinapyl alcohol, were detected following gas chromatography-mass spectrometry analysis of the soluble portion.<sup>7</sup> Thereafter, the cellulose-rich insoluble residue and lignin-rich precipitates were evaluated as substrates of enzyme-mediated bioconversion and PL materials, respectively.



## Enzyme-mediated bioconversion of cellulose-rich insoluble residue

The hydrolysis yield was enhanced significantly following the HCW treatment (from 16.9% to 63.8%; Fig. 1a). The WRVs were one of the general indicators for evaluating the enzyme accessibility to the cellulose component of the insoluble residue. As shown in Fig. 1b, the WRV of the insoluble residue was clearly enhanced relative to that of the untreated wood (from 163% to 223%). In addition, Simon's staining method using DO dye was employed to predict the enzyme accessibility to the cellulose component.<sup>22</sup> As a result, the DO adsorption was also enhanced in the insoluble residue. The WRVs and DO dye adsorption results both indicated that the cellulase enzyme had sufficient accessibility to the cellulose component in the insoluble residue (Fig. 1b). Lignin is known to have a significant detrimental effect on enzymatic hydrolysis because of its unproductive binding to the enzyme. To suppress this negative effect, BSA was incorporated into the substrates (*i.e.*, insoluble residue and untreated wood flour) to block the lignin prior to enzymatic hydrolysis.<sup>23–25</sup> The addition of BSA enhanced the insoluble residue conversion yields, indicating that unproductive binding occurred in the insoluble residue. This result could be interpreted as the promotion of a condensation reaction involving residual lignin.<sup>25,26</sup> Compared with the effect of the acidic

pretreatment, the influence of BSA addition was restricted because of the limited lignin condensation reaction.

UV microscopy measurements were performed at a wavelength of 280 nm to observe the distribution of lignin within the cell wall (Fig. 1c and d). The UV absorbance at the secondary wall (SW) in fiber and vessel regions decreased in the insoluble residue compared with the untreated wood. The blackness of the line profile on the adjacent fiber and vessel was plotted to determine the lignin concentration in each morphological region. In the untreated wood, the middle lamella cell corner (ML<sub>CC</sub>) region had the highest UV absorption, while the SW in the fiber and vessel regions exhibited one-third to one-fourth the absorption intensity of the ML<sub>CC</sub> region; this result was consistent with what was observed in typical wood.<sup>27</sup> In contrast, for the insoluble residue, the UV absorbance at the SW (especially in the fiber region) was low compared to that of the ML<sub>CC</sub>, indicating that preferential delignification occurred in the SW. This phenomenon has been observed following other thermochemical treatments owing to the high resistance of condensed lignin-rich substances in the middle lamella.<sup>28,29</sup> The surface morphology of the insoluble residue observed using SEM revealed that the fiber surface was covered with amorphous layers, which are considered part of the compound middle lamella (Fig. 1e). In contrast, numerous small pores were visible on the surface of the lumen (arrows in Fig. 1f); the decomposed compounds would be eluted through these pores on the lumen surface.

Because cellulose is distributed throughout the SW, the preferential delignification from SW enhanced the enzymatic hydrolysis of the cellulose component despite the fact that the lignin content was similar in the insoluble residue (25.3% = 10/39.5) and untreated wood (25.3%).

## Photoluminescence properties of lignin-rich precipitates

The lignin-rich precipitates were dissolved in dimethyl sulfoxide (DMSO) at 0.1 mg mL<sup>-1</sup>, and their optical properties were evaluated based on their UV-vis absorption and PL spectra. The spectra of MWL, which is considered as the representative structure of natural lignin, are presented for comparison. The UV-vis absorption spectra of the precipitates and MWL solutions contained a peak at approximately 280 nm, which is characteristic of lignin (Fig. S2†). Their PL spectra excited at 320 nm are shown in Fig. 2a, and both species exhibited clear PL. However, the precipitates have much higher PL intensity, with the peak maximum at longer wavelength (378 nm) compared with MWL (369 nm). Although the chemical structures of MWL and the precipitates are similar, the precipitates had lower molecular weight (Table S1†), which led to a more uniform dissolution and dispersion in DMF. When the precipitates were dissolved in different solvents (*e.g.*, high-polarity DMSO or low-polarity CHCl<sub>3</sub>), the PL spectra differed; the PL intensity of the precipitates in CHCl<sub>3</sub> was lower than that in DMF (Fig. 2b and S2†). Similar PL quenching phenomena are observed in various types of lignin, including MWL, kraft lignin, and sulfite lignin, and the extent of the quenching can be explained according to the distances between the two proximal

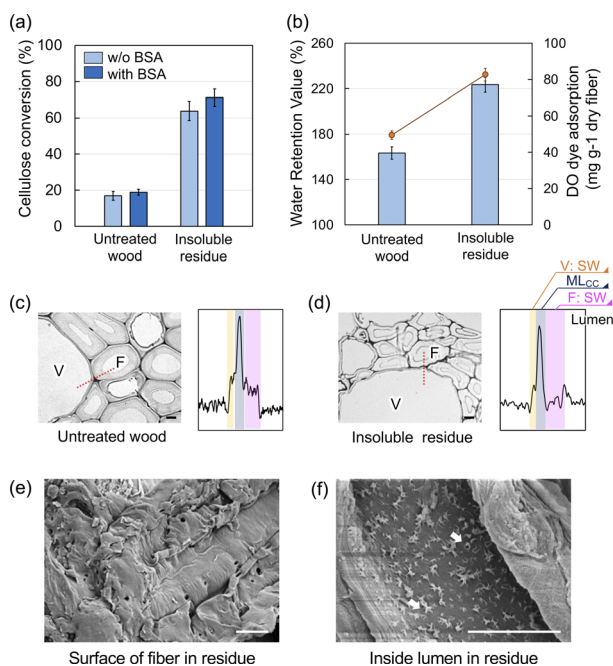
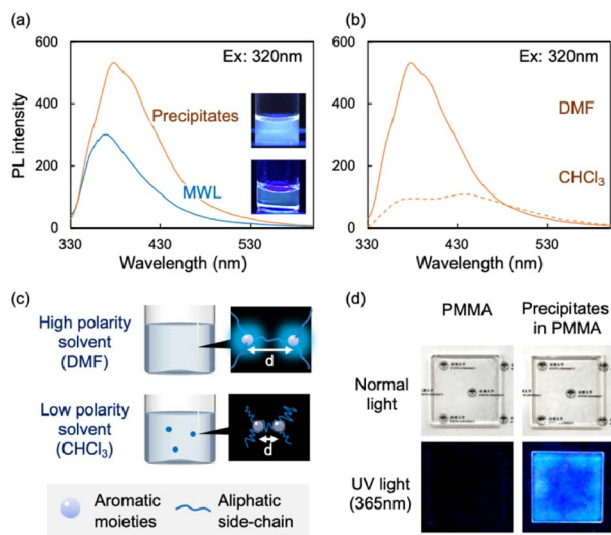


Fig. 1 (a) Enzymatic hydrolysis of untreated wood and insoluble residue after HCW treatment; (b) evaluation of cellulose accessibility to cellulose component based on WRVs (bar, left) and DO dye adsorption of substrates (circles, right); UV micrographs of (c) untreated wood and (d) insoluble residues at 280 nm (left), and the profile of the red dotted lines (right); (e and f) SEM micrographs of insoluble residue, (e) surface morphology and (f) inside the lumen (scale bar = 5  $\mu$ m). BSA = bovine serum albumin; DO = Direct Orange; F = fiber; ML<sub>CC</sub> = middle lamella at cell corner; SW = secondary wall; V = vessel.





**Fig. 2** (a) PL spectra of MWL and precipitates in DMSO ( $0.1 \text{ mg mL}^{-1}$ ) solution excited at 320 nm; (b) PL spectra of precipitates in DMSO and  $\text{CHCl}_3$  at  $0.1 \text{ mg mL}^{-1}$ ; (c) schematic diagram of quenching in low-polarity solvent ( $\text{CHCl}_3$ ); (d) photographs of PMMA films with and without precipitates on quartz under normal light (top) and UV light (365 nm, bottom).

aromatic moieties (luminophores) (Fig. 2c).<sup>6</sup> In other words, the lignin PL quenching can be suppressed if the average distance between luminophores remains short. When the solution containing the precipitates was mixed with a PMMA solution and casted onto quartz glass slides to obtain a transparent film, as shown in Fig. 2d and S3,<sup>†</sup> the lignin-containing precipitates exhibited clear PL both in the solutions and in the films at the macroscopic level.

In summary, the cell wall components of beech wood were selectively fractionated using a semi-flow HCW treatment into cellulose-rich insoluble residues and lignin-rich precipitates. The enzyme-mediated bioconversion of the cellulose components in the insoluble residue was enhanced by improving enzyme accessibility. In addition, the precipitates showed clear PL properties that could be controlled by altering the chromophore distances. Therefore, the semi-flow HCW treatment represents an effective biorefinery approach to promote the comprehensive utilization of all cell wall components.

### Influence of 2-naphthol on hydrolysis and photoluminescence

To mitigate the re-condensation of lignin, various quantities of 2-naphthol (0%, 4%, 8%, or 16%) were incorporated into the beech wood flour before the hot-compressed water treatment. Table 2 shows the yields of each fraction isolated from beech wood following the semi-flow HCW treatment with and without the addition of 2-naphthol. No significant differences were observed. Approximately 40% was isolated as the insoluble residue, and 6.3–6.9% was retrieved as precipitates (with similar chemical compositions). Although it is quite difficult to accurately determine the exact mass balance of 2-naphthol in each fraction, the incorporated amounts in the precipitates were small (see FT-IR analysis). Most of the 2-naphthol was either

**Table 2** Yields of each fraction obtained from Japanese beech treated by semi-flow hot-compressed water with 2-naphthol

Loading of 2-naphthol (%)	Yield of each fraction (%)		
	Insoluble residue	Precipitates	Water-soluble portion
0	$39.5 \pm 0.6$	$6.8 \pm 0.7$	$53.7 \pm 0.3$
4	$41.5 \pm 2.1$	$6.3 \pm 0.8$	$52.2 \pm 1.4$
8	$40.1 \pm 0.5$	$6.7 \pm 1.0$	$53.1 \pm 0.7$
16	$38.8 \pm 0.6$	$6.9 \pm 1.2$	$54.3 \pm 1.8$

incorporated into the insoluble residues or the water-soluble portion. Next, the enzyme-mediated hydrolysis of the insoluble residue and the PL properties of the precipitates were investigated.

The cellulose conversion yields following enzymatic hydrolysis increased slightly as the 2-naphthol loading increased (Fig. 3). Notably, the incorporation of BSA prior to hydrolysis did not enhance the conversion yields for the insoluble residue with 16% 2-naphthol added. This result indicated that the unproductive binding between lignin and the enzyme did not have a significant impact. The addition of 2-naphthol mitigated the re-condensation as expected, and the negative effect of lignin on enzymatic hydrolysis was avoided. Unproductive binding was observed in BSA-added enzymatic saccharification of the residue obtained in the systems containing 4% and 8% 2-naphthol. This suggested that the addition of 4% or 8% 2-naphthol was not sufficient because of the limited contact between the carbocation of the lignin and the added 2-naphthol. The WRVs increased slightly (Fig. 3) and were correlated with the conversion yields. In terms of the lignin distribution within the cell walls, a similar preferential delignification from the SW was observed by UV microscopy for the insoluble residue obtained following HCW treatment with 2-naphthol (Fig. S4<sup>†</sup>).

The PL spectra of precipitates obtained after HCW treatment with different loading amounts of 2-naphthol are shown in Fig. 4. When DMF solutions containing the precipitates were excited at 320 nm, all samples showed clear PL with a peak at 380 nm. As the loading of 2-naphthol increased, the PL intensity of the precipitate solutions increased (Fig. 4b). When the PL

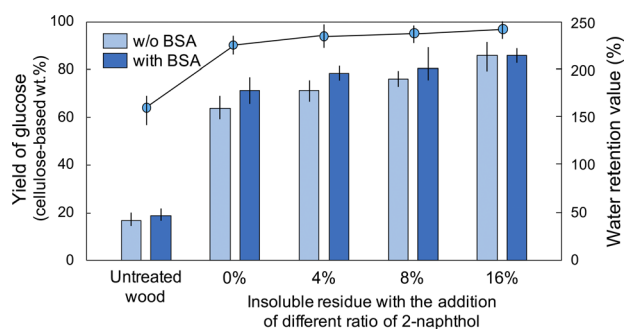


**Fig. 3** Enzymatic hydrolysis of untreated wood and insoluble residue treated by HCW with the addition of 2-naphthol (0%, 4%, 8%, or 16%) with and without BSA (bars), and their WRVs (circles).



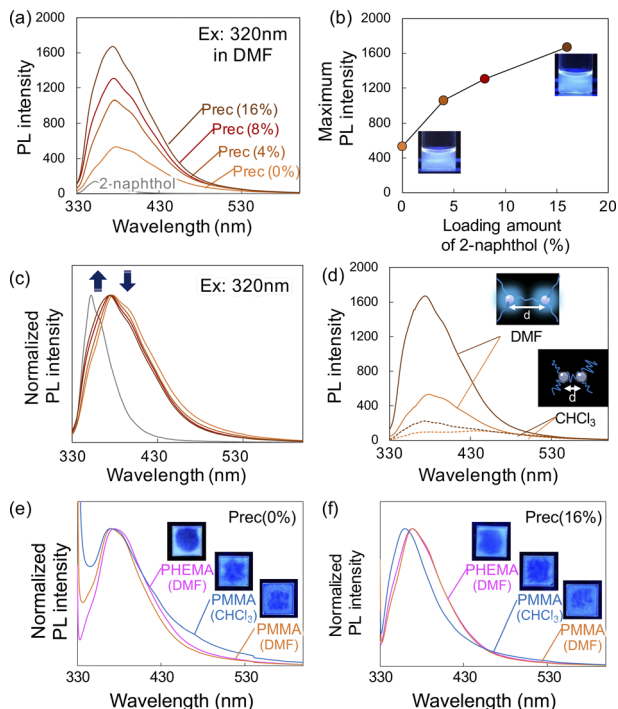


**Fig. 4** (a) PL properties of precipitates from Japanese beech treated by HCW with and without 2-naphthol (in DMSO,  $0.1 \text{ mg mL}^{-1}$ , excited at 320 nm). For comparison,  $0.01 \text{ mg mL}^{-1}$  of 2-naphthol solution is also shown. (b) Correlation between the amount of added 2-naphthol and the maximum PL intensity. (c) Normalized PL spectra: (d) PL spectra of precipitates dissolved in DMF or  $\text{CHCl}_3$  at  $0.1 \text{ mg mL}^{-1}$ , (e) normalized PL spectra of Prec(0%)-incorporated film, and (f) normalized PL spectra of Prec(16%)-incorporated film (excitation wavelength = 320 nm).

spectra were normalized, the peak maximum did not shift; however, the spectral profile changed slightly toward shorter wavelengths (*i.e.*, slight decrease at 400 nm and slight increase at 350 nm; Fig. 4c). These high PL intensities and changes in the spectral patterns with different 2-naphthol loadings were also observed at excitation wavelengths of 280 and 350 nm (Fig. S5†). Comparing the fluorescence lifetimes of the precipitates revealed that the Prec(16%) DMF solution was 3.16 ns, which was slightly longer than that of the Prec(0%) DMF solution ( $\tau = 2.84 \text{ ns}$ ), but much shorter than that of 2-naphthol ( $\tau = 4.56 \text{ ns}$ ) (Table S2†). The PL spectra of Prec(16%) and Prec(0%) in DMF and  $\text{CHCl}_3$  are shown in Fig. 4e. Quenching of the PL in  $\text{CHCl}_3$  was also observed in Prec(16%), although the PL intensity was still higher than that in Prec(0%). Because 2-naphthol has relatively low polarity, its incorporation into lignin molecules would promote the dispersion of lignin in  $\text{CHCl}_3$ . Both precipitates could be dispersed in polymers to prepare transparent films. Various solvents (DMF and  $\text{CHCl}_3$ ) and polymers (PMMA and PHEMA) were used to prepare a series of transparent films, which all exhibited PL properties under UV light. In the case of Prec(0%), the PL spectrum differed depending on the characteristics of the polymer (*i.e.*, PMMA and PHEMA) and the solvent (*i.e.*, DMF and  $\text{CHCl}_3$ ), indicating that the medium influenced the PL properties (Fig. 4e). In the case of Prec(16%), the PL spectrum varied slightly in different solvents (Fig. 4f).

The vibrations of chemical bonding of precipitated lignin were detected using FT-IR (Fig. 5). As shown in Scheme 2, the naphthalene-ring structure is considered to be retained through the incorporation into lignin, suggesting that the incorporated 2-naphthol structure in precipitated lignin would exhibit the similar peaks to those of 2-naphthol monomer. As a result, the IR spectra of Prec(0%) and Prec(16%) were similar, and no peaks derived from 2-naphthol were observed in Prec(16%), indicating that the 2-naphthol content was below the limit of detection. The enlarged fingerprint region (Fig. 5b) revealed slight shifts in Prec(16%) at 1460, 1420, and  $1368 \text{ cm}^{-1}$  compared with MWL and Prec(0%). Considering that these peaks are derived from the aromatic structure,<sup>30</sup> the shifts indicated that the stiffness of the aromatic rings were influenced by the incorporation of 2-naphthol. According to the integrated area of the peak at  $1270 \text{ cm}^{-1}$  (corresponding to a G-type ring), the MWL contained significantly more G-type ring moieties than the precipitates. This low level of G lignin in Prec(0%) was attributed to the preferential delignification from the SW, which was rich in S-type lignin (Fig. 1d).

These results suggest that the incorporation of 2-naphthol prior to HCW treatment enhanced the digestibility of the cellulose component in the residue by suppressing (i) lignin recondensation and (ii) unproductive binding between lignin and enzyme. In contrast, the PL intensity of the precipitates was significantly enhanced, suggesting that 2-naphthol bound to the lignin side-chains influenced the PL properties of the lignin. Regarding the optimal loading concentration of 2-naphthol, 16% would be sufficient in terms of hydrolyzability due to its negligible improvement by the incorporation of BSA prior to the enzymatic hydrolysis. In contrast, the PL intensities may increase at higher loading concentration of 2-naphthol. Given that the improvement of PL intensity between Prec(8%) and Prec(16%) is less than that between Prec(0%) and Prec(4%), the loading more than 16% 2-naphthol would not yield significant advantages.

### Influence of 2-naphthol versus phenol on hydrolysis of residue and photoluminescence of precipitates

To confirm the effect of 2-naphthol addition, phenol (*i.e.*, the simplest phenolic compound) was also impregnated into beech wood prior to the HCW treatment, and their effects were compared. No significant differences were observed in terms of the yields of each fraction (Table 3). Similarly, there were no appreciable changes in the enzyme-mediated hydrolysis of the insoluble residue following the phenol-incorporated HCW treatment (Fig. 6a), which indicated that the phenol did not act as a carbocation scavenger during the HCW treatment. The increased hydrolysis yields after BSA addition are consistent with this conclusion. The PL properties of the precipitated lignin were similar to those of Prec(0%) (Fig. 6b and S6†). Taken together, these results indicate that 2-naphthol is an effective additive because it can serve as a carbocation scavenger; however, not all phenolic compounds have a similar benefit. Furthermore, the effect of 2-naphthol on aquatic plants was discussed in the introduction, but since 2-naphthol itself does



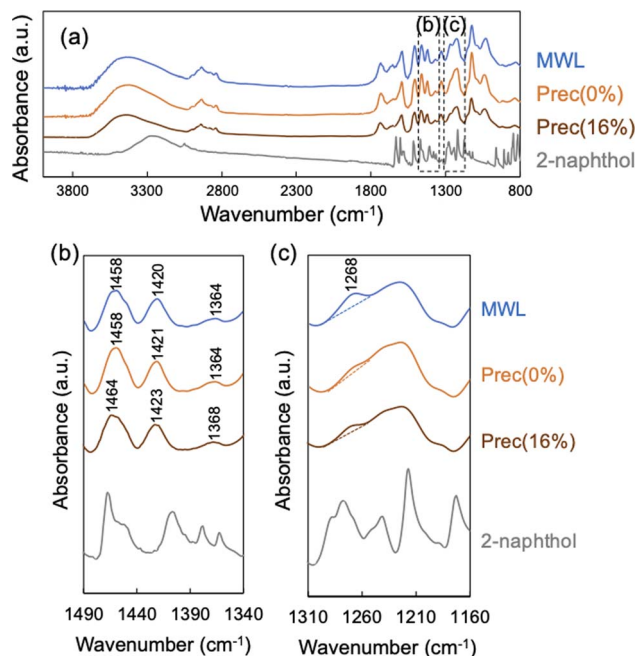


Fig. 5 (a) FT-IR spectra of precipitates from Japanese beech treated *via* HCW with and without 2-naphthol (16%); enlarged spectra from (b) 1490 to 1340  $\text{cm}^{-1}$  and (c) from 1310 to 1160  $\text{cm}^{-1}$ . The spectra of MWL and 2-naphthol are also shown for comparison.

not exist as a monomer but is incorporated into lignin, it is expected to have no ecological impact if the unreacted portion is properly recovered.

Table 3 Yields of each fraction from Japanese beech treated by semi-flow hot-compressed water with and without 2-naphthol or phenol

Added chemicals	Yield of each fraction (%)		
	Insoluble residue	Precipitates	Water-soluble portion
Without	39.5 ± 0.6	6.8 ± 0.7	53.7 ± 0.3
2-Naphthol (16%)	38.8 ± 0.6	6.9 ± 1.2	54.3 ± 1.8
Phenol (16%)	39.2 ± 1.5	6.4 ± 2.3	54.4 ± 1.2

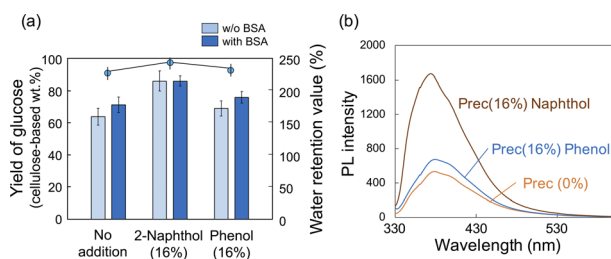


Fig. 6 Comparison of the effects of adding 2-naphthol or phenol (16%): (a) enzymatic hydrolysis and WRVs of insoluble residues from Japanese beech treated by HCW with and without 16% phenol or 2-naphthol; (b) PL spectra of precipitates dissolved in DMSO at 0.1  $\text{mg mL}^{-1}$  and excited at 320 nm.

## Conclusions

Cellulose-rich insoluble residues and lignin-rich precipitates were fractionated from beech wood using a semi-flow HCW treatment. The cellulose component in the residue underwent high conversion *via* enzymatic saccharification owing to the improved enzyme accessibility. Meanwhile, the lignin-rich precipitates in DMF solution showed clear PL that could be controlled according to the chromophore distances. In addition, 2-naphthol was impregnated into the wood prior to the HCW treatment and served as a carbocation scavenger under acidic conditions. Both the digestibility of the cellulose in the residue and the PL properties of the lignin precipitates were improved significantly as the 2-naphthol loading increased. The results presented herein indicate that the described semi-flow HCW treatment comprises an effective biorefinery approach to the comprehensive utilization of woody biomass cell wall components. Furthermore, the impregnation of 2-naphthol imparts a dual benefit in terms of the utilization of both cellulose and lignin. The effectively converted glucose can be further transformed into value-added products *via* a well-established sugar platform; this process is applicable in a wide range of fields, such as pharmaceuticals, food, fibers, and functional materials. In contrast, the lignin precipitates showed useful photoluminescence properties both in solution and in films, indicating that the fractionated lignin has significant potential as a feedstock for valuable functional materials, such as fluorescence reagents, fluorescence sensors, and optical wavelength conversion agents.

## Data availability

The data supporting this article have been included as part of the ESI.†

## Author contributions

MT conceived, designed, and conducted the experiments. MT and YO analyzed the experimental data and drafted the manuscript. All authors read and approved the final manuscript.

## Conflicts of interest

There are no conflicts to declare.

## Acknowledgements

This work was supported by KAKENHI (Grant No. 22K14927) and JST FOREST Program (Grant No. JPMJFR2277).

## References

- Z. Zhou, D. Liu and X. Zhao, *Renewable Sustainable Energy Rev.*, 2021, **146**, 111169.
- J. H. Lora, *Monomers, Polymers and Composites from Renewable Resources*, Elsevier, Amsterdam, 2008.
- H. Sadeghifar and A. Ragauskas, *Polymers*, 2020, **12**, 1134.



- 4 K. Shikinaka, M. Nakamura and Y. Otsuka, *Polymer*, 2020, **190**, 122254.
- 5 Y. Zhang and M. Naebe, *ACS Sustain. Chem. Eng.*, 2021, **9**, 1427–1442.
- 6 M. Takada, Y. Okazaki, H. Kawamoto and T. Sagawa, *ACS Omega*, 2022, **7**, 5096–5103.
- 7 X. Lu, K. Yamauchi, N. Phaiboonsilpa and S. Saka, *J. Wood Sci.*, 2009, **55**, 367–375.
- 8 M. Takada, E. Minami and S. Saka, *J. Supercrit. Fluids*, 2018, **133**, 566–572.
- 9 M. Takada, E. Minami, K. Yamauchi, H. Kawamoto and S. Saka, *Holzforschung*, 2017, **71**, 285–290.
- 10 H. Rabemanolontsoa, K. Yoshimizu and S. Saka, *J. Chem. Technol. Biotechnol.*, 2016, **91**, 1040–1047.
- 11 S. Nakagame, R. P. Chandra and J. N. Saddler, in *ACS Symposium Series*, 2011, vol. 1067, pp. 145–167.
- 12 M. Wayman and J. H. Lora, *Tappi*, 1978, **61**, 55–57.
- 13 T. Pielhop, G. O. Larrazábal, M. H. Studer, S. Brethauer, C.-M. Seidel and P. Rudolf von Rohr, *Green Chem.*, 2015, **17**, 3521–3532.
- 14 Q. Zhou, M. Lei, J. Li, K. Zhao and Y. Liu, *J. Chromatogr. A*, 2016, **1441**, 1–7.
- 15 S. Yang, M. Gao and Z. Luo, *Chem. Eng. J.*, 2014, **256**, 39–50.
- 16 M. J. Selig, S. Viamajala, S. R. Decker, M. P. Tucker, M. E. Himmel and T. B. Vinzant, *Biotechnol. Prog.*, 2007, **23**, 1333–1339.
- 17 B. S. Donohoe, S. R. Decker, M. P. Tucker, M. E. Himmel and T. B. Vinzant, *Biotechnol. Bioeng.*, 2008, **101**, 913–925.
- 18 A. Björkman, *Sven. Papperstidn.*, 1956, **59**, 477–485.
- 19 R. Chandra, S. Ewanick, C. Hsieh and J. N. Saddler, *Biotechnol. Prog.*, 2008, **24**, 1178–1185.
- 20 M. Takada, J. Wu, H. Kawamoto, D. Rio and J. Saddler, *Sustainable Energy Fuels*, 2022, **6**, 3788–3793.
- 21 G. Gellerstedt, in *Methods in Lignin Chemistry*, ed. S. Y. Lin and C. W. Dence, 1994, pp. 487–497.
- 22 R. Bura, R. Chandra and J. Saddler, *Biotechnol. Prog.*, 2009, **25**, 315–322.
- 23 C. Huang, X. Jiang, X. Shen, J. Hu, W. Tang, X. Wu, A. Ragauskas, H. Jameel, X. Meng and Q. Yong, *Renewable Sustainable Energy Rev.*, 2022, **154**, 111822.
- 24 J. Liu, J. Wu, Y. Lu, H. Zhang, Q. Hua, R. Bi, O. Rojas, S. Renneckar, S. Fan, Z. Xiao and J. Saddler, *Bioresour. Technol.*, 2023, **367**, 128276.
- 25 B. Yang and C. E. Wyman, *Biotechnol. Bioeng.*, 2006, **94**, 611–617.
- 26 Y. Jia, C. Yang, B. Shen, Z. Ling, C. Huang and X. Li, *Bioresour. Technol.*, 2021, **319**, 124225.
- 27 P. Whiting and D. A. I. Goring, *J. Wood Chem. Technol.*, 1981, **1**, 111–122.
- 28 M. Takada, Y. Tanaka, E. Minami and S. Saka, *Holzforschung*, 2016, **70**, 1047–1053.
- 29 M. Takada, E. Minami and H. Kawamoto, *ACS Omega*, 2021, **6**, 20924–20930.
- 30 O. Faix, in *Methods in Lignin Chemistry*, ed. S. Y. Lin and C. W. Dence, Springer Berlin Heidelberg, 1992, pp. 233–241.

